Selective Regulation of xSlo Splice Variants During *Xenopus* Embryogenesis

Manuel Kukuljan,[1] Alison Taylor,[2] Hilary Chouinard,[2] Patricio Olguín,[1] Cecilia V. Rojas,[3] and Angeles B. Ribera[2]

[1]*Programa de Fisiología y Biofísica, Instituto de Ciencias Biomédicas, Facultad de Medicina, Universidad de Chile, Independencia 1027, Santiago, Chile;* [2]*Department of Physiology and Biophysics, University of Colorado Health Sciences Center, Denver, Colorado 80262; and* [3]*Instituto de Nutrición y Tecnología de los Alimentos, Universidad de Chile, Av. J.P. Alessandri 5540, Santiago, Chile*

Kukuljan, Manuel, Alison Taylor, Hilary Chouinard, Patricio Olguín, Cecilia V. Rojas, and Angeles B. Ribera. Selective regulation of xSlo splice variants during *Xenopus* embryogenesis. *J Neurophysiol* 90: 3352–3360, 2003. First published July 16, 2003; 10.1152/jn.00398.2003. Calcium-activated potassium channels regulate excitability of the adult nervous system. In contrast, little is known about the contribution of calcium-activated potassium channels to excitability of the embryonic nervous system when electrical membrane properties and intracellular calcium levels show dramatic changes. Embryonic *Xenopus* spinal neurons exhibit a well-characterized developmental program of excitability that involves several different currents including calcium-activated ones. Here, we show that a molecular determinant of calcium-activated potassium channels, xSlo, is expressed during *Xenopus* embryogenesis even prior to differentiation of excitable tissues. Five different xSlo variants are expressed in embryonic tissues as a consequence of alternative exon usage at a single splice site. One of these variants, xSlo59, is neural-specific, and its expression is limited to late stages of neuronal differentiation. However, expression of the four other variants occurs in both muscle and neurons at all stages of development examined. Electrophysiological analysis of recombinant xSlo channels reveals that the xSlo59 exon serves as a gain-of-function module and allows physiologically relevant levels of membrane potential and intracellular calcium to activate effectively the resultant channel. These results suggest that xSlo59 channels play a unique role in sculpting the excitable membrane properties of *Xenopus* spinal neurons.

INTRODUCTION

The Slo gene encodes the pore-forming α subunit of large-conductance calcium-activated potassium (BK) channels (Atkinson et al. 1991; Butler et al. 1993). Neuronal activity produces both membrane depolarization and intracellular calcium elevations, resulting in activation of Slo potassium channels and repolarization of the membrane potential. The calcium sensitivity of Slo channels plays an important role in determining its physiological role.

Even though a single gene encodes Slo channel α subunits, hundreds of different Slo transcripts and protein products can be generated as a result of extensive alternative splicing (Adelman et al. 1992; Atkinson et al. 1991; Butler et al. 1993; Navaratnam et al. 1997; Rosenblatt et al. 1997; Tseng-Crank et al. 1994). Alternative exon usage regulates channel properties including both voltage and calcium sensitivities (Lagrutta et al. 1994; Rosenblatt et al. 1997; Saito et al. 1997). Alternative splicing may account for tissue specific differences in the functional properties of BK channels that allow fine tuning of cellular excitability. (Latorre et al. 1989).

Given the significant functional consequences of alternative exon usage, expression of specific variants may be subject to extensive regulation. Indeed, the hormonal state of the organism determines whether the STREX-2 exon within the large carboxyl-terminus of rSlo is expressed (Xie and McCobb 1998). Inclusion of the STREX-2 exon alters the calcium and voltage sensitivities of the channel, and, thereby, modulates firing properties of chromaffin cells and secretion of epinephrine (Lovell and McCobb 2001). Inclusion of specific alternative exons in Slo transcripts thus matches cellular excitability to physiological requirements.

Given that alternative exon usage of Slo transcripts is regulated and affects cellular excitability, it is possible that developmental regulation of alternative splicing of the Slo gene may occur in embryonic neurons as they acquire their mature functional phenotype. Primary neurons of the developing spinal cord of the frog, *Xenopus laevis*, have served as a powerful system for addressing questions regarding developmental regulation of excitability (Spitzer and Ribera 1998). *Xenopus* spinal neurons display profound changes in cellular excitability as they progress from the electrically silent state to neurons that fire stereotypic brief sodium-dependent action potentials (Spitzer and Ribera 1998). Further, calcium-activated potassium currents have been recorded from these neurons (Blair and Dionne 1985; O'Dowd et al. 1988). Moreover, the properties of calcium-activated currents in these neurons show developmental regulation (Blair and Dionne 1985; O'Dowd et al. 1988).

In view of these considerations, we cloned the *Xenopus* Slo gene (xSlo) and analyzed alternative exon usage during the period when the action potential of primary spinal neurons undergoes dramatic developmental regulation (1–2 days in vivo). We report evidence for four alternative splice variants. One of the alternative variants, xSlo59, demonstrates neural-specific and developmentally specific expression. Inclusion of this exon in xSlo subunits renders recombinant channels sensitive to physiological levels of membrane depolarization and intracellular calcium.

METHODS

Screening of cDNA libraries, DNA sequencing and analysis

Isolation of *Xenopus* Slo (xSlo) cDNAs was accomplished by a combination of DNA library screening and reverse transcription-polymerase chain reaction (RT-PCR) amplification of mRNA. For screening of cDNA libraries, ^{32}P-labeled (New England Nuclear, Boston, MA) random-primed probes (Prime-It Kit, Stratagene, La Jolla, CA) were generated initially using the 3′ end of mSlo (kindly provided by Dr. Lawrence Salkoff, Dept. of Anatomy and Neurobiology, Washington University) and subsequently from 5′ ends of previously isolated xSlo partial cDNAs. Phage DNA was transferred to nitrocellulose filters and hybridized to ^{32}P-labeled probes following standard procedures (Burger and Ribera 1996; Ribera 1990; Ribera and Nguyen 1993). Isolated clones were sequenced over both strands using the Sanger dideoxy method using either radiolabeled or fluorescent precursors. DNA sequences were read and analyzed using Gel Reader (CBS Scientific, Del Mar, CA) and DNASTAR software (Madison, WI).

RNA isolation and RT-PCR of xSlo cDNA

Cellular mRNA was isolated from whole embryos or cultured dissociated neural plate cells by homogenization and proteinase K treatment as previously described (Ribera 1990). cDNA synthesis was performed using oligo dT (Gibco BRL, Gaithersburg, MD)and Superscript II RT (GIBCO-BRL). The cDNA was used as input for subsequent PCRs using degenerate oligonucleotide primers that recognized regions of Slo that are highly conserved across species. The PCR conditions were five cycles at 95° for 2 min (denaturation), 48° for 2 min (annealing), 72° for 2 min (extension) followed by 35 cycles at 95° for 2 min, 58° for 2 min, and 72° for 2 min 45 s. Two different negative control reactions were run. The first tested for amplification of genomic DNA and consisted of preparing a RT reaction tube but omitting the RT enzyme. The second negative control tested for contamination in the PCR and consisted of preparing a RT reaction tube without RNA. Both of these negative controls were subjected to the two rounds of PCR as described in the preceding text. PCR products were gel purified and cloned (TA Cloning kit, Invitrogen, Carlsbad, CA). DNA sequencing confirmed their identity as *Slo* cDNAs.

Construction of an xSlo cDNA containing the entire coding region

The entire coding region of xSlo was contained within five overlapping cDNA clones. In a 5′ to 3′ order, these clones were xSlo4 (N terminus to beginning of S2), xSlo26 (S0–S3), xSlo25 (S3–S6), xSlo6 (S6–S10), and xSlo2 (S9 to 3′UTR). A single clone containing a continuous complete coding region (xSlo0) was assembled from the five overlapping cDNAs by a combination of further RT-PCR and attachment of clones using appropriate restriction sites. In brief, xSlo25 and xSlo6 were joined at a common *Hin*dIII site to yield clone 25/6. A clone encompassing xSlo4, xSlo26, xSlo25, and a portion of xSlo6 was generated by RT-PCR and called R4. R4 was joined to 25/6 at a shared EcoN1 restriction site to yield clone R4/25/6. R4/25/6 was joined to xSlo2 at a shared *Bgl*II restriction site to yield the clone, xSlo, that contained the entire coding region, 105 bp of 5′UTR, and 730 bp of 3′UTR. DNA sequencing confirmed that restricted fragments had been ligated to each other in frame and without introduction of base substitutions. Once the cDNAs had been assembled into a single clone, the entire open reading frame was resequenced.

Identification of xSlo splice variants

RT-PCR was used to examine the possibility of alternative splicing in the region 3′ to S6. RNA was isolated and cDNA was reverse transcribed, as described in the preceding text. Forward and reverse PCR primers were designed that were 5′ and 3′, respectively, to potential sites of alternative splicing; in each case, an internal control for the effectiveness of the primer set was provided by amplification of a band corresponding to the product expected if no alternative insert existed at a particular site. In all, seven potential sites were examined. Four alternative inserts found for the site corresponding to mouse site 2 (Butler et al. 1993) or human site 2 (Tseng-Crank et al. 1994) were cloned and sequenced. In this study, we refer to this position as *site 2*.

Whole-mount in situ hybridization

The nonradioactive detection method (Ferreiro et al. 1993; Harland 1991) was followed with minor modifications as previously described (Burger and Ribera 1996). Embryos were produced by adult *Xenopus* breeding pairs or in vitro fertilization and staged according to Nieuwkoop and Faber (1967). cRNA probes were synthesized in the presence of digoxigenin-labeled UTP (Boehringer-Mannheim). Antisense and sense control probes corresponded to a region common to all xSlo transcripts; the antisense probe is referred to as the universal probe. For each stage examined, in situ hybridization experiments were repeated at least three times. Whole-mount embryos were either cleared in Murray's solution (2:1 benzyl benzoate:benzyl alcohol) or embedded in plastic (JB-4 embedding kit; Polysciences, Warrington, PA). Fifteen- to 30-μm sections were counterstained (e.g., methyl green, eosin) and photographed with Kodak Ektachrome 160T film. Slides were digitized using a Nikon Cool Scanner and composite figures were prepared using Adobe PhotoShop software.

Electrophysiology

The entire coding region of *xSlo* was subcloned into pGEMHE (generously provided by Dr. E. Liman) (Liman et al. 1991). The resultant clone was called pGHExSlo. In addition, the four alternative inserts found at *site 2* were introduced separately into pGHExSlo. The resulting recombinant constructs were linearized with *Nhe*I and capped sense RNA was generated in vitro (mMessage mMachine, Ambion, Austin, TX). Oocytes were surgically removed, defolliculated, and injected with 0.5–50 ng of RNA as described previously (Burger and Ribera 1996; Ribera and Nguyen 1993) and incubated at 18° in ND-96 solution [which contained (in mM) 96 NaCl, 2 KCl, 1.8 $CaCl_2$, 1 $MgCl_2$, and 5 HEPES, pH7.5]. Excised macropatch recordings were carried out 2–10 days post injection. Electrodes were pulled from soft-glass to obtain resistances of 0.3–0.7 MΩ when filled with 100 mM potassium methanesulfonate (K-MES), 5 HEPES, pH 7.6 with KOH. Oocytes were placed in a chamber containing 100 mM K-MES, 5 HEPES, pH 7.2 with KOH, $CaCl_2$, and calcium chelators to obtain the free calcium concentrations in the desired range (EGTA for the submicromolar range, EGTA and HEDTA for the 2- to 20-μM range, and NTA-HEDTA for the 60- to 80-μM range). The appropriate concentrations of $CaCl_2$ and each chelator were determined using Maxchelator software, developed by Dr. C. Patton (www.stanford.edu/~cpatton/maxc.html); actual free calcium concentrations were directly measured using a calcium-selective electrode calibrated with commercially available standards (World Precision Instruments, Sarasota, FL). Dithiothreitol (10 mM) was added to the bath solution to prevent the time-dependent rundown and shift in activation curves described for other Slo channels (DiChiara and Reinhart 1997). Vitelline membranes were manually removed, inside-out macro patch-clamp configurations were established, and capacitative currents were electronically compensated. Changes of the free calcium concentration in the bath solution were achieved using a gravity-driven perfusion system. PCLAMP6 (Axon Instruments, Union City, CA) programs were used to execute voltage protocols and evaluate tail current amplitudes (see following text).

For analysis of steady-state voltage dependence of activation, we

analyzed tail currents. The protocol consisted of changing the membrane potential to a series of activating potentials ranging between –90 and +160 mV in 10-mV increments and then returning to the holding potential of –90 mV. Because symmetrical potassium solutions were used (E_K = 0 mV), inward tail currents were recorded when the membrane potential was returned to the holding value of –90 mV. Each membrane patch was subjected to several different intracellular [Ca^{2+}], ranging between 0.6 μM and 1 mM, and tail currents were recorded in the presence of each of these different solutions. For data obtained from each excised membrane patch, we normalized tail current amplitudes to the maximum tail current amplitude (I_{max}) obtained in the presence of the maximum intracellular [Ca^{2+}]. Thus I_{max} was determined in the presence of 1 mM intracellular Ca^{2+}. Activation curves were constructed by plotting the normalized tail current amplitude (I/I_{max}) as a function of the activating membrane potential. Given that we measured tail currents that were obtained at the same voltage (−90 mV), I_{max} and I/I_{max} reflect G_{max} and G/G_{max}, respectively. The equation $G/G_{max} = G_{max}/1 + \exp([V_{1/2} - V]/k)$ was fit to the tail current data (G_{max}, maximal conductance; $V_{1/2}$, voltage of half-activation; k, slope factor). Calcium sensitivity was evaluated by plotting the value of $V_{1/2}$ as a function of the intracellular [Ca^{2+}].

For experiments examining properties of *site 2* variants, we expressed the five identified variants in oocytes from the same batch to minimize the possibility that changes in functional properties might reflect variability between batches of oocytes rather than different intrinsic properties of each variant.

Data are presented as means ± SE. Student's *t*-test was used to assess statistical significance. P values ≤0.05 used to indicate statistical significance.

RT-PCR analysis of variant expression in tissue and culture RNA

RNA was isolated from dissected tissues of neural tube 1 and 2-day embryos (St. 18–24) and neural plate cultures. Neural plate stage (St. 15) cultures were prepared as described previously (Ribera and Spitzer 1989) except that three to five neural plates were cultured per 60-mm culture dish. Reverse and forward primers flanking *site 2* were designed (forward, 5′ gccatctgccttgctgagctg 3′/1563–1579; reverse, 5′ catgcagtgggctatt atcaggtgatg 3′/2706–2680). The reverse primer was used in the RT reaction as well as the first round of PCR. The forward primer was used in the first round of PCR as well as in the second nested PCR. For the nested PCR, five different reverse primers were designed and each recognized a specific *site 2* variant (0Rev, 5′ aggctgatggctgctcatcttcaag 3′; 15Rev, 5′ caggcaaggaagggtgaggagg 3′; 56Rev, 5′ gcggatggacatcttggaataaataag 3′; 59Rev, 5′ gcggatggacatcttggaataaataag 3′; 99Rev, 5′ gcctgtggatacttaatctatgttc 3′). Further, when any of these reverse nested primers was used with the forward primer, PCR products of similar size (ca. 400 bp) were generated. Accordingly, five separate nested PCRs followed each first round of PCR. The nested PCR products were cloned and sequenced to confirm their identity. RT-PCR analyses of xSlo variant expression in dissected tissues and neural plate cultures were repeated at least four times.

RESULTS

Isolation of a Xenopus Slo cDNA

The Slo gene encodes the α subunit of BK-type calcium-activated potassium channels. We identified the *Xenopus* orthologue of Slo (xSlo) by performing standard cDNA library screening in combination with RT-PCR. We isolated five overlapping partial cDNAs. The five overlapping cDNAs were assembled into a single clone containing a 3,588-bp open reading frame that codes for a 1,196 amino acid protein (Fig. 1). We refer to this sequence as xSlo0.

Several in-frame ATGs are found in the 5′ region of Slo genes from other species (Atkinson et al. 1991; Butler et al. 1993). However, we found only a single in-frame ATG in the 5′ region of xSlo0. This ATG was in the context of a canonical Kozak sequence (Kozak 1987), having the critical A/G and G at the −3 and +4 positions, respectively. Accordingly, we designated this ATG as the start codon. The predicted amino acid sequence of xSlo0 showed high identity with Slo subunits identified in other vertebrate species. The greatest identities were found across the regions encompassing the four hydrophobic domains known as S7–S10 (~90%) and the putative transmembranous segments (S0–S6; ~95%). The amino-terminus displayed the highest degree of divergence, being only ~60% identical to the analogous region of other vertebrate Slo subunits. A region found in mSlo1, known as the "calcium bowl" (Schreiber and Salkoff 1997), strongly influences calcium sensitivity. The calcium bowl consists of two linear sequences of 6 and 21 amino acids separated by one variant amino acid and is identical in mouse, fly, worm, and human Slo. This region was also exactly conserved in xSlo0 (Fig. 1, amino acids 914–941). Another critical region for Slo channel function is the subunit association domain known as BK-T1 (Quirk and Reinhart 2001). This region was also conserved in xSlo0, suggesting that xSlo subunits can coassemble with invertebrate and other vertebrate Slo subunits. Because phosphorylation can modulate BK channel function (Weiger et al. 2002), it was also of interest to examine the xSlo sequence for potential phosphorylation sites. xSlo0 contains 14 consensus sites for A or C kinase-dependent phosphorylation.

xSlo transcripts are present in excitable tissues of the embryo

Because of our interest in excitability during embryonic stages, we determined the expression pattern of the xSlo0 gene in *Xenopus* embryos by performing whole-mount in situ hybridization. In these studies, we used the universal probe that recognized a region common to xSlo0 and possible splice variants (see METHODS). Embryos ranging in age between 1 and 3 days (St. 18–36) were examined because of the well-known changes in excitability that occur during this time (Spitzer and Ribera 1998). We found that excitable tissues of the developing embryo expressed xSlo mRNA in a spatially and temporally dynamic pattern (Figs. 2 and 3). xSlo transcripts were detected in both the somites and neural tube of 1day embryos. Within the nervous system, xSlo expression demonstrated a dorsal restriction and was thus expressed centrally in regions dedicated to processing of sensory information. Six hours later, xSlo expression appeared segmentally within the somites. At this time, xSlo expression was detected in a primary sensory organ, the trigeminal ganglion. By 2 days, other primary sensory organs (e.g., otic vesicle, eye) also began to express the xSlo gene. Within the retina, xSlo transcripts localized to an internal layer (Fig. 3*E*). In the developing otic vesicle, xSlo transcripts were abundant near the apical surface (Fig. 3*F*).

Alternative splicing of xSlo during embryonic development

In several species, alternative splicing of the Slo gene occurs and generates both molecular and functional heterogeneity of

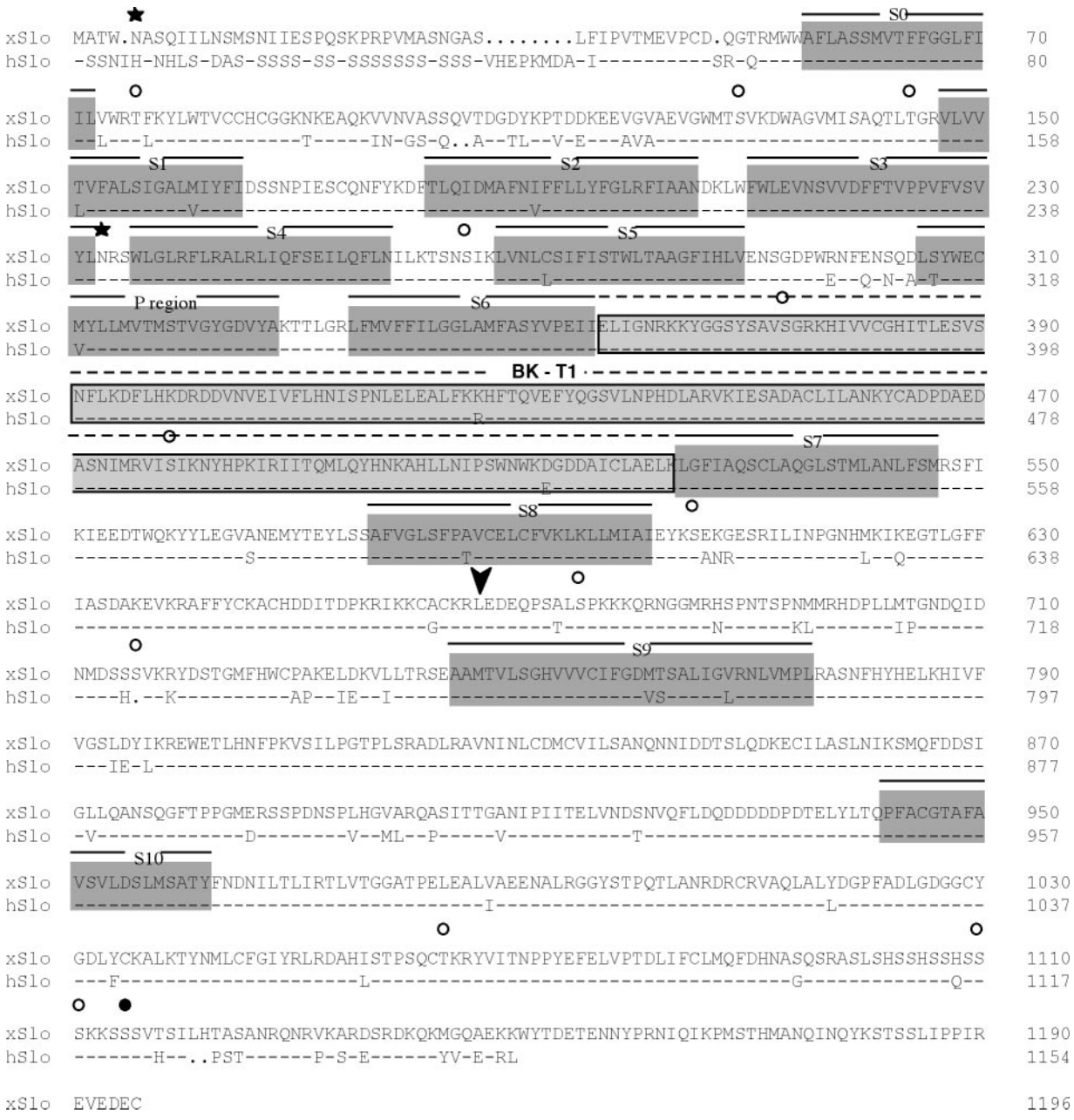

FIG. 1. Alignment of xSlo and hSlo amino acid sequences. Hydrophobic segments, S0–S10, and the putative pore, P region, are indicated by dark gray shading and overlying solid lines. The association domain, BK-T1 (Quirk and Reinhart 2001), is indicated by light gray shading and an overlying dotted line. Potential phosphorylation sites in xSlo0 are indicated by either filled (A kinase) or open (C kinase) circles; a star designates a putative *N*-glycosylation site in the amino-terminal region. An overlying arrowhead points to the site of alternative splicing studied in this paper; the splice site interrupts a codon for leucine (see Fig. 4).

Slo peptides (Atkinson et al. 1991; Butler et al. 1993; Rosenblatt et al. 1997; Tseng-Crank et al. 1994). We were particularly interested in the possibility that splicing might occur within the region encoding the large cytoplasmic tail; splicing within this region has been shown to affect calcium sensitivity (e.g., Lagrutta et al. 1994; Saito et al. 1997). Using the positions at which alternative splicing occurs within dSlo, mSlo, rSlo, and hSlo transcripts as a vantage point, we tested for alternative splicing at seven different sites within the region coding for the large cytoplasmic tail of xSlo0 (Fig. 4*A*). We designed PCR primers that flanked the seven potential splice junctions and performed RT-PCR using 1- or 2-day embryo RNA as input. Despite the fact that seven potential sites were examined, we detected splice variants at only one site, known as *site 2* in mSlo (Butler et al. 1993). In rSlo, alternative splicing at this same site results in the introduction of the so-called STREX exons that confer novel functional properties on Slo channels in a hormone-dependent manner (Saito et al.1997; Xie and McCobb 1998).

Our RT-PCR analyses identified four alternative exons at *site 2*, coding for inserts that added either 15, 56, 59, or 99 amino acids to the xSlo0 backbone. The 56 and 59 amino acid variants shared 60% amino identity with rat STREX-1 and -2 exons (Xie and McCobb 1998). The 56 and 59 amino acid

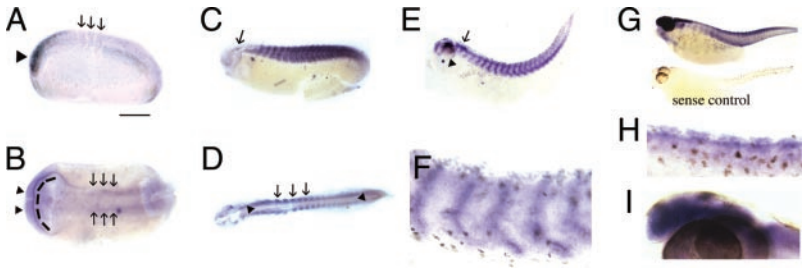

FIG. 2. Development dynamically regulates expression of the xSlo gene in excitable tissues. xSlo transcripts were detected in whole-mount preparations of *Xenopus* embryos by in situ hybridization (see METHODS). In all panels, anterior is to the left. Lateral views of embryos are presented, except in *B* and *D*, which contain dorsal views. *A*: at 25 h, xSlo transcripts were detected in the neural tube (▲) and somites (→ point to 3 adjacent somites). Scale Bar: 100 μm. *B*: by viewing the embryo of *A* dorsally, neural (▲) and somitic (→) expression of xSlo was evident along the anterior-posterior axis. [The anterior lining of the archenteron (- - -) nonspecifically collected reaction product.] *C*: at 31 h, xSlo expression was abundant in somites and began to appear in the trigeminal ganglion (→). *D*: viewing the embryo of *C* dorsally revealed xSlo expression throughout the neuraxis (▲) and segmentally within the somites (→). *E*: at 46 h, xSlo transcripts concentrated in mid-somite regions. Anteriorally, xSlo expression appeared in the otic vesicle (→) and eye (▲). *F*: magnified view of the trunk region of the embryo in *E*. *G*: in both antisense (*top*) and sense control (*bottom*) 3 day embryos, pigment cells appeared brown. xSlo expression transcripts were found throughout the somites. In contrast, within the neural tube, xSlo transcripts localized to dorsal regions. *H*: magnified view of xSlo expression in the trunk region of the 3d embryo in *G*. *I*: within the head of the 3-day embryo of *G*, xSlo transcripts were detected in the eye and brain.

variants differ by only 3 amino acids (LIY). We did not find any inserts that corresponded to these three amino acids only even though our screen did not bias against their identification.

The presence of STREX-like exons in frogs, turtles, birds, and mammals and their absence in flies and worms suggest that STREX exons are a vertebrate specialization. In contrast, neither the 15 nor 99 amino acid insert displayed sequence similarity with *site 2* alternative exons found in other species and thus may be unique to frogs.

Expression of site 2 alternative exons

We performed RT-PCR analyses to determine the expression patterns of *site 2* variants within excitable tissues of the developing *Xenopus* embryo. After the RT reaction, we carried out five PCRs in parallel. Each PCR used a common forward primer but a different reverse primer that was specific for each splice variant. Further, the reverse primers were designed so that the PCR products generated for each variant would be of similar size. DNA sequencing confirmed the specific identity of each PCR product.

To examine excitable tissues of the developing embryo, we isolated RNA from either the somites (precursors of skeletal muscle) or neural plate (presumptive spinal cord) of the trunk of Stage 18–20 embryos (20–22 h). We found that the xSlo0, xSlo15, xSlo56, and xSlo99 variants were present in RNA isolated from either somitic or neural plate tissue (Fig. 4*B*). In striking contrast, the xSlo59 variant was not expressed by somitic tissue. However, we detected expression of the xSlo59 variant in the neural plate, indicating that the expression of this variant was neural-specific.

Alternative splicing generates functional heterogeneity

To study the functional properties of channels coded for by the xSlo gene, we performed heterologous expression experiments using the *Xenopus* oocyte system. In initial two-electrode voltage-clamp studies, we found that the outward currents induced by heterologous expression of xSlo0 cRNA in oocytes were voltage dependent and sensitive to TEA and charybdotoxin, classic blockers of BK current (data not

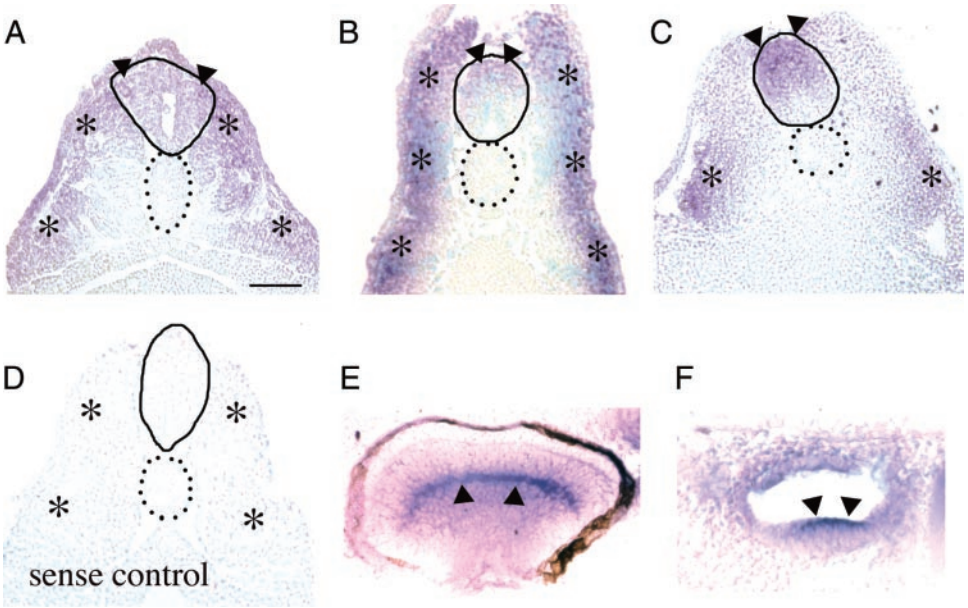

FIG. 3. xSlo transcripts localize to both embryonic neuronal and muscle cells. Whole-mount embryos were processed as for Fig. 2 and then embedded in plastic and sectioned (10–30 μm). *A* and *D*, *B* and *C*, and *E* and *F* are sections from 1, 2, and 3 day embryos, respectively. In all panels, dorsal is up. In *A–D*, the neural tube/spinal cord is encircled by —; the notochord is outlined by · · · and * lie on the flanking somites. *A*: in 1-day embryos, xSlo expression was detected in the neural tube (▲) and somites (*). Scale bar: *50* μm. *B*: in the anterior portion of the trunk of 2-day-old embryos, xSlo transcripts concentrated in the lateral portion of the somites (*) and dorsal neural tube (▲). *C*: in 3-day-old embryos, xSlo expression continued to localize to dorsal regions of the neural tube (▲) and ventrally within the somites (*). *D*: 1-day sense control. *E*: in the retina, xSlo transcripts localized to an internal layer (▲). The pigmented epithelium that envelops the retina appeared brown. *F*: xSlo transcripts were detected near the apical side (▲) of the otic vesicle.

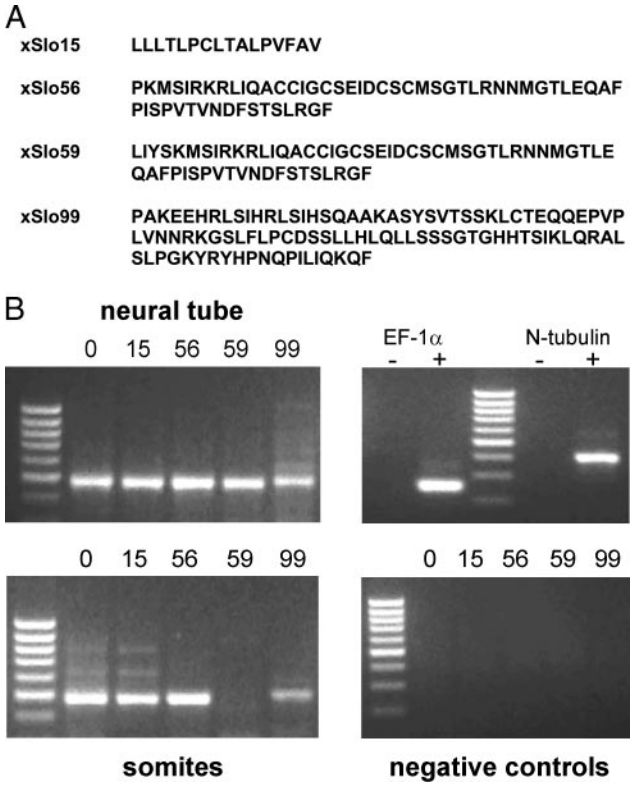

FIG. 4. Alternative splicing produces molecularly diverse xSlo transcripts. *A*: 4 alternative exons—xSlo15, xSlo56, xSlo59, and xSlo99—were detected at *site 2* by RT-PCR analysis of RNA isolated from 2-day-old embryos. The predicted amino acid sequences of the 4 alternative inserts at splice site 2 are shown. *B*: 3 of the alternative *site 2* exons–xSlo15, xSlo56, and xSlo99—were expressed in both the spinal cord and somites of the developing embryo. In contrast, the xSlo59 exon was detected only in the developing spinal cord (*left*). RT-PCR analysis of constitutively expressed EF-1α and neuronal-specific N-tubulin expression (*top right*) served as positive controls for RNA and neural tissue loading. When reverse transcriptase was omitted, xSlo PCR products were not generated, indicating that the PCR products reflected mRNA expression (*bottom right*). Similar results were obtained from $\geq$4 experiments for each variant and tissue examined.

shown). To analyze quantitatively the properties of channels generated by xSlo0 and the four *site 2* variants, we recorded currents from excised inside-out macropatches of oocytes injected with the different cRNAs (Fig. 5). We first analyzed calcium-dependent properties by exposing the intracellular surface of the membrane patch to different concentrations of calcium. For example, for patches excised from oocytes expressing xSlo0 cRNA, exposing the intracellular patch membrane to 2.7 μM calcium allowed depolarization to activate more current in response to depolarization than when the patch was exposed to 0.6 μM calcium (Fig. 5).

We next compared the voltage-dependent properties of the different variants. We found that the xSlo59 variant was most sensitive to depolarization (Fig. 5, *B–D*). In the presence of 72 μM "intracellular" calcium, ~30 mV less depolarization was required to activate half of the xSlo59 versus xSlo0 conductance (Fig. 5*C*). Moreover, over a wide range of intracellular calcium concentrations (0.6–1000 μM), the voltage of half-maximal activation ($V_{1/2}$), was consistently more negative for xSlo59 versus xSlo0 and the other variant channels (Fig. 5*D*). With respect to calcium and voltage sensitivities, xSlo15, xSlo56, and xSlo99 channels behaved more similarly to xSlo0 than to xSlo59 channels. Moreover, the xSlo56 variant, which differs from the xSlo59 variant by only four amino acids, displayed values of $V_{1/2}$ that differed significantly from those of xSlo59 at "intracellular" calcium concentrations of 0.6, 16, 72, and 1,000 μM (Fig. 5*D*; $P \leq 0.001$; values did not differ for 2.7 μM "intracellular" calcium). Taken together, these data indicate that physiological levels of calcium and membrane potential effectively activate xSlo59 channels. Thus both functional properties as well as neural-specific expression uniquely characterize the xSlo59 variant.

Development regulates expression of site 2 variants in Xenopus spinal neurons

Alternative splicing at *site 2* serves as a mechanism to modify the functional properties of xSlo subunits. For example, inclusion of the xSlo59 exon confers physiologically relevant calcium- and voltage-dependent properties on xSlo channels. Moreover, the fact that this variant is neural-specific raises the possibility that expression of this gain-of-function exon is under selective regulation. To test this possibility further, we next examined how expression of xSlo0 and the *site 2* variants was regulated during development. We focused on the stage of development (~1–2 days in vivo; 6–24 h in vitro) during which spinal neurons undergo a well-characterized change in membrane excitability that results in dramatic shortening of the impulse duration (Spitzer and Lamborghini 1976).

We isolated RNA from neural plate cultures or whole embryos at two developmental time points. One day in vivo and 6 h in vitro correspond to stages when spinal neurons fire long-duration impulses. In contrast, at 2 days in vivo or 24 h in vitro the action potential of spinal neurons has matured to a brief 1- to 2-ms duration event. RT-PCR analysis for each variant indicated that at 24 h in vitro and 2 days in vivo, all five variants were expressed. However, at 6 h in vitro, we did not detect expression of the xSlo59 variant. Similarly, in vivo, xSlo59 expression is upregulated at 2 compared with 1 day. Thus the neural-specific xSlo59 is developmentally upregulated. The xSlo56 variant also displays developmentally upregulated expression. However, this latter variant is not neural specific as is xSlo59 (Fig. 4).

DISCUSSION

Extensive alternative exon usage characterizes the Slo gene in species as diverse as worms and humans (Atkinson et al. 1991; Butler et al. 1993; Jones et al. 1998; Navaranatan et al. 1997; Rosenblatt et al. 1997; Tseng-Crank et al. 1994; Wang et al. 2001). In flies and mice, the combination of identified alternative Slo exons allows for hundreds of different proteins. Even though the functional significance of each identified Slo exon as well as their combinatorial usage has not yet been established, inclusion of specific exons in mature transcripts significantly alters physiologically relevant channel properties, such as voltage and calcium sensitivities (Lagrutta et al. 1994; Rosenblatt et al. 1997; Saito et al. 1997; Xie and McCobb 1998). Further, expression of functionally diverse Slo gene products can modify critical parameters of cellular excitability, such as activation threshold (Saito et al. 1997; Xie and McCobb 1998). Despite the enormous diversity of Slo gene products, we identified only four alternative exons that are included

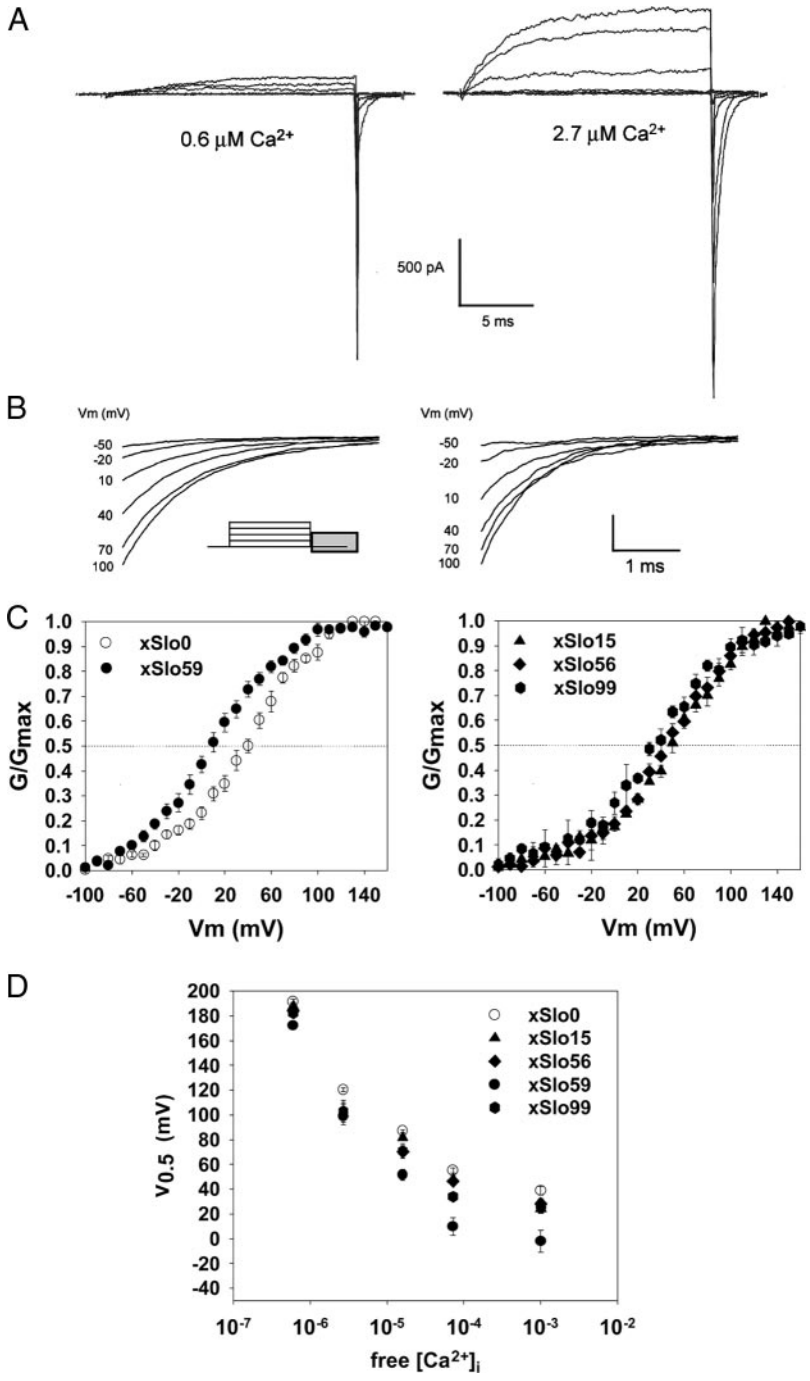

FIG. 5. xSlo0 and xSlo59 variants code for functionally distinguishable calcium-activated potassium channels. *A*: injection of xSlo0 mRNA into *Xenopus* oocytes induced expression of potassium channels that are sensitive to calcium. Membrane patches were excised from oocytes and their "intracellular" surfaces were exposed to different concentrations of calcium (e.g., 0.6 μM, *left;* 2.7 μM, *right*). In the presence of 2.7 μM calcium, depolarization activated larger amplitude currents than when the same patch was exposed to 0.6 μM calcium. *B*: Slo channels produced by the xSlo59 variant differed functionally from those generated by xSlo0 mRNA. Specifically, xSlo59 channels generated currents that required less depolarization for activation. Tail currents were recorded at –90 mV after activation of currents by depolarizing voltage steps to potentials ranging between –50 and +100 mV (*inset*). The concentration of free Ca^{2+} in the solution bathing the intracellular surface of the membrane patch was 72 μM. *C*: conductance-voltage analysis of currents generated by xSlo0 and the xSlo59 variant. The $V_{1/2}$ of xSlo59 channels was ~30 mV more negative than that of xSlo0 channels, allowing physiological levels of depolarization to activate more effectively xSlo59 vs. xSlo0 channels. *D*: $V_{1/2}$ obtained for each xSlo variant were plotted as a function of the intracellular free calcium concentration. Over a wide range of intracellular calcium concentrations, less depolarization was required to activate xSlo59 vs. xSlo0 or other *site 2* variant channels. $V_{1/2}$ values for xSlo56 and xSlo59 channels were significantly different at calcium concentrations of 0.6, 16, 72, and 1,000 μM ($P \leq 0.001$). Mean ± SE values are presented; *n* ranged between 3 and 7 for each data point.

at a single site (A) in xSlo transcripts expressed during embryonic development of the *Xenopus* embryo. While it is possible that more extensive splicing of xSlo occurs during later preand postmetamorphic stages, the limited number of xSlo gene products found during embryogenesis contrasts with the diversity of neuronal excitability phenotypes noted at these stages (Spitzer and Ribera 1998).

Sites for insertion of alternative exons have been conserved during evolution (Atkinson et al. 1991; Butler et al. 1993; Jones et al. 1998; Navaranatan et al. 1997; Rosenblatt et al. 1997; Tseng-Crank et al. 1994). In contrast, the predicted amino acid sequences of alternative exons generally show little homology across species. However, a notable exception is a subset of cysteine-rich exons (STREX) found at *site 2*, between domains S8 and S9 of the large cytoplasmic carboxyl-terminus (Saito et al. 1997; Xie and McCobb 1998). STREX exons exist in a wide range of vertebrate species (e.g., frog, chicks, and rat), but have not yet been identified in invertebrate species such as worms or flies. Any novel function or modulation that these exons impart on the resultant protein may have evolved as vertebrate specializations. Do STREX exons add new functions to Slo channels? We found that the xSlo59 exon acts as a gain-of-function module. Inclusion of the xSlo59 exon renders the resultant channel more sensitive to intracellular calcium and membrane depolarization. These changes predict efficient activation of xSlo59 channels at physiologically relevant levels of intracellular calcium and membrane voltage. With re-

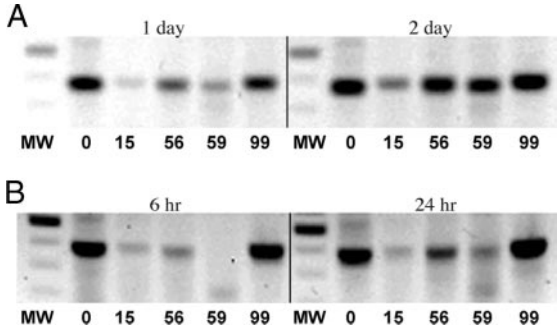

FIG. 6. Development regulates expression of the xSlo59 *site 2* variant. Expression of *site 2* variants was examined at different stages of development by RT-PCR. The RT-PCR analyses were repeated ≥4 times, and similar results were obtained each time. *A*: examination of 1- and 2-day embryo RNA indicated that the xSlo59 variant was upregulated in vivo. *B*: similarly, for RNA isolated from neural plate cultures, RT-PCR analysis indicated that the xSlo59 variant was expressed at 24 (*right*) but not 6 h (*left*) after plating. In contrast, all other variants were expressed at both times in culture.

spect to voltage sensitivity, the effects of xSlo59 are similar to those observed when STREX-2 is included in rSlo channels (Saito et al. 1997; Xie and McCobb 1998). Additionally, inclusion of these exons modulates the sensitivity of Slo channels to phosphorylation (Erxleben et al. 2002; Tian et al. 2001).

The sequences of the xSlo56 and xSlo59 exons differ only by the inclusion of three additional amino acids (LIY) and a codon change that substitutes serine for proline (Fig. 4). STREX-1 and -2 exons differ also by the inclusion of the amino acid sequence LIY (Xie and McCobb 1998). Despite these minimal differences, xSlo59 adds physiologically significant calcium and voltage sensitivities to xSlo channels while xSlo56 has only subtle effects. Given the minimal sequence differences between xSlo56 and xSlo59 (and STREX-1 and -2), it is surprising that they differ significantly in how they alter xSlo channel function.

An additional indication that expression of the xSlo59 exon has important functional consequences is that it displays a highly regulated expression pattern with respect to tissue, while xSlo0 and the other *site 2* variants do not (Fig. 4). xSlo0 and the other *site 2* variants are expressed in both muscle and neural tissue. In contrast, xSlo59 shows neural-specific expression. In addition, xlo59 and the related xSlo56 variants display a developmentally upregulated expression pattern (Fig. 6). Thus these two variants are more robustly expressed at later stages of neuronal differentiation after the period when transient calcium elevations occur spontaneously in *Xenopus* spinal neurons (Holliday and Spitzer 1990). An impressive regulatory mechanism for expression of STREX exons has also been observed for rSlo. In adrenal chromaffin cells, steroid hormones tightly regulate expression of the STREX exons, which in turn alter firing properties and secretion of epinephrine (Lai and McCobb 2002; Lovell and McCobb 2001; Xie and McCobb 1998).

Expression of critical sodium and potassium channel genes occurs during neurulation in the *Xenopus* embryo (Armisén et al. 2002; Burger and Ribera 1996; Ribera 1990,1996). Thus acquisition of the mature electrophysiological phenotype of *Xenopus* spinal neurons requires new transcription during postmitotic stages of differentiation (Ribera and Spitzer 1989). Our current results suggest that in addition to transcription, developmentally regulated alternative splicing fine tunes the electrical properties of differentiated neurons. This complexity in mechanisms may go even further to cell specific variations as demonstrated for the expression of a variety of voltage-activated potassium channels that yield an apparently homogeneous functional phenotype (Ribera 1996). The relative simplicity of xSlo transcript processing during embryonic stages may provide an entry point for in vivo analysis of splicing mechanisms.

Primary amphibian neurons initially fire long-duration, calcium-dependent action potentials, which are subsequently converted to brief, sodium-dependent spikes (Spitzer and Lamborghini 1976). Long-duration impulses allow significant elevations of intracellular cytosolic and nuclear calcium (Holliday et al. 1991). These calcium transients provide signals necessary for subsequent elaboration of key neuronal properties, including neurite initiation, formation of neuron-myocyte contacts, accumulation of GABA-like immunoreactivity, and acceleration of potassium current kinetics (Bixby and Spitzer 1984; Desarmenien and Spitzer 1991; Gu and Spitzer 1995; Henderson et al. 1984; Holliday and Spitzer 1990; Holliday et al. 1991). Previous evidence indicates that several different types of voltage-gated potassium channels (e.g., Kv1, Kv2, Kv3) play important roles in action potential repolarization as spinal neurons mature (Blaine and Ribera 2001; Ribera 1996; Vincent et al. 2000). The present work extends these findings by raising the possibility that another class of channels, calcium-activated potassium channels, also participate in developmental regulation of the duration of spinal neuron action potentials.

Our RT-PCR developmental analyses indicate that expression of the xSlo59 variant is neural-specific. Further, xSlo59 expression shows a dramatic increase after the period of initial excitability when neurons fire long-duation impulses (Fig. 6). At later stages, inclusion of the xSlo59 exon would result in channels that enhance repolarization of action potentials and generation of afterhyperpolarizations and consequently modulate the firing properties of spinal neurons. The increased sensitivity to intracellular calcium of xSlo59 channels could serve as a powerful negative feedback system and attenuate elevations of intracellular calcium during periods of neuronal activity. In addition, such channels could have dramatic effects on the firing properties of mature neurons. Indeed, Sun and Dale (1998) reported that application of the large-conductance calcium-activated potassium channel blocker, iberiotoxin, to mature neurons led to more rapid firing rates. These latter findings suggest that developmentally regulated expression of xSlo channels, especially ones with higher sensitivity to intracellular calcium, could contribute to the observed changes in firing properties of these neurons.

The xSlo56 variant is also developmentally upregulated. However, this variant is not expressed in a neural-specific manner, making it difficult to determine whether developmental upregulation occurs in all tissues or a restricted subset. The analyses presented in Fig. 6 examined expression in RNA extracted from the entire embryo or from neural plate cultures, both of which contain neurons as well as other excitable and nonexcitable cells.

Calcium signals in excitable tissues regulate stage-specific expression of several genes, including genes encoding ion channels. For example, the developmentally regulated expression of calcium-activated potassium channels in ascidian mus-

cle depends on the activity of voltage-gated calcium channels, presumably through the increase of intracellular calcium levels (Dallman et al. 1998). Further, calcium/calmodulin-dependent protein-kinase-mediated processes regulate alternative splicing of Slo transcripts (Xie and Black 2001). These findings raise the possibility that cellular electrical activity controls the selection of alternative exons in xSlo transcripts, such as xSlo59. These findings add new temporal and mechanistic dimensions to the role of calcium-activated potassium channels as feedback elements for excitability.

DISCLOSURES

This work was supported by National Institutes of Health Grants NS-25217 (A. B. Ribera) and TW-01314 (M. Kukuljan, A. B. Ribera), Fondo Nacional de Ciencia y Technogia Grants 1961084 (M. Kukuljan) and 1970363 (C. V. Rojas), and Fundación G. Puelma (M. Kukuljan).

REFERENCES

Adelman JP, Shen KZ, Kavanaugh MP, Warren RA, Wu YN, Lagrutta A, Bond CT, and North RA. Calcium-activated potassium channels expresed from cloned complementary DNAs. *Neuron* 9: 209–216, 1992.

Armisén R, Fuentes R, Olguín P, Cabrejos ME, and Kukuljan M. Repressor element-1 silencing transcription/neuron-restrictive silencer factor is required for neural sodium channel expression during development of *Xenopus*. *J Neurosci* 22: 8347–8351, 2002.

Atkinson NS, Robertson GA, and Ganetzky B. A component of calcium-activated potassium channels encoded by the *Drosophila* slo locus. *Science* 253: 551–555, 1991.

Bixby JL and Spitzer NC. Early differentiation of vertebrate spinal neurons in the absence of voltage-dependent Ca^{2+} and Na^{+} influx. *Dev Biol* 106: 89–96, 1984.

Blaine JT and Ribera AB. Kv2 channels form delayed-rectifier potassium channels in situ. *J Neurosci* 21: 1473–1480, 2001.

Blair LA and Dionne VE. Developmental acquisition of Ca^{2+}-sensitivity by K^{+} channels in spinal neurones. *Nature* 315: 329–331, 1985.

Burger C and Ribera AB. *Xenopus* spinal neurons express Kv2 potassium channel transcripts during embryonic development. *J Neurosci* 16: 1412–1421, 1996.

Butler A, Tsunoda S, McCobb DP, Wei A, and Salkoff L. mSlo, a complex mouse gene encoding the "maxi" calcium-activated potassium channels. *Science* 26: 221–224, 1993.

Chandy KG and Gutman GA. Nomenclature for mammalian potassium channel genes. *Trends Pharmacol Sci* 14:434, 1993.

Dallman JE, Davis AK, and Moody WJ. Spontaneous activity regulates calcium-dependent K^{+} current expression in developing ascidian muscle. *J Physiol* 511: 683–693, 1998.

Desarmenien MG and Spitzer NC. Role of calcium and protein kinase C in development of the delayed rectifier potassium current in *Xenopus* spinal neurons. *Neuron* 7: 797–805, 1991.

DiChiara TJ and Reinhart PH. Redox modulation of hslo Ca^{2+}-activated K^{+} channels. *J Neurosci* 17: 4942–4955, 1997.

Erxleben C, Everhart AL, Romeo C, Florance H, Bauer MB, Alcorta DA, Rossie S, Shipston MJ, and Armstrong DL. Interacting effects of N-terminal variation and strex exon splicing on slo potassium channel regulation by calcium, phosphorylation, and oxidation. *J Biol Chem* 277: 27045–2752, 2002.

Ferreiro B, Skoglund P, Bailey A, Dorsky R, and Harris WA. XASH1, a *Xenopus* homologue of *Achaete scute*: a proneural gene in anterior regions of the vertebrate central nervous system. *Mech Dev* 40: 25–36, 1993.

Gu X and Spitzer NC. Distinct aspects of neuronal differentiation encoded by frequency of spontaneous Ca^{2+} transients. *Nature* 375: 784–787, 1995.

Harland RM. In situ hybridization: an improved whole-mount method for *Xenopus* embryos. *Methods Cell Biol* 36: 685–695, 1991.

Henderson LP, Smith MA, and Spitzer NC. The absence of calcium blocks impulse-evoked release of acetylcholine but not de novo formation of functional neuromuscular synaptic contacts in culture. *J Neurosci* 4: 3140–3150, 1984.

Holliday J, Adams RJ, Sejnowski TJ, and Spitzer NC. Calcium-induced release of calcium regulates differentiation of cultured spinal neurons. *Neuron* 7: 787–796, 1991.

Holliday J and Spitzer NC. Spontaneous calcium influx and its roles in differentiation of spinal neurons in culture. *Dev Biol* 141: 13–23, 1990.

Jones EMC, Laus C, and Fettiplace R. Identification of Ca^{2+}-activated K^{+} channel splice variants and their distribution in the turtle cochlea. *Proc R Soc Lond B Biol Sci* 265: 685–692, 1998.

Kozak M. At least six nucleotides preceding the AUG initiator codon enhance translation in mammalian cells. *J Mol Biol* 196: 947–950, 1987.

Lagrutta A, Shen KZ, North RA, and Adelman JP. Functional differences among alternatively spliced variants of Slowpoke, a *Drosophila* calcium-activated potassium channel. *J Biol Chem* 269: 20347–20351, 1994.

Lai GJ and McCobb DP. Opposing actions of adrenal androgens and glucocorticoids on alternative splicing of Slo potassium channels in bovine chromaffin cells. *Proc Natl Acad Sci USA* 99: 7722–7727, 2002.

Latorre R, Oberhauser A, Labarca P, and Alvarez O. Varieties of calcium-activated potassium channels. *Annu Rev Physiol* 51: 385–399, 1989.

Liman ER, Hess P, Weaver F, and Koren G. Voltage-sensing residues in the S4 region of a mammalian K^{+} channel. *Nature* 353: 752–756, 1991.

Lovell PV and McCobb DP. Pituitary control of BK potassium channel function and intrinsic firing properties of adrenal chromaffin cells. *J Neurosci* 21: 3429–3442, 2001.

Navaratnam DS, Bell TJ, Tu TD, Cohen EL, and Oberholtzer JC. Differential distribution of Ca^{2+}-activated K^{+} channels splice variants among hair cells along the tonotopic axis of the chick cochlea. *Neuron* 19: 1077–1085, 1997.

Nieuwkoop PD and Faber J. Normal Table of *Xenopus laevis.* Amsterdam: Daudin, 1967.

O'Dowd DK, Ribera AB, and Spitzer NC. Development of voltage-dependent calcium, sodium, and potassium currents in *Xenopus* spinal neurons. *J Neurosci* 8: 792–805, 1988.

Quirk JC and Reinhart PH. Identification of a novel tetramerization domain in large conductance K(ca) channels. *Neuron* 32: 13–23, 2001.

Ribera AB. A potassium channel gene is expressed at neural induction. *Neuron* 5: 691–701, 1990.

Ribera AB. Homogeneous development of electrical excitability via heterogeneous ion channel expression. *J Neurosci* 16: 1123–1130, 1996.

Ribera AB and Nguyen DA. Primary sensory neurons express a Shaker-like potassium channel gene. *J Neurosci* 13: 4988–4996, 1993.

Ribera AB and Spitzer NC. A critical period of transcription required for differentiation of the action potential of spinal neurons. *Neuron* 2: 1055–1062, 1989.

Rosenblatt KP, Sun Z-P, Heller S, and Hudspeth AJ. Distribution of Ca^{2+}-activated K^{+} channels isoforms along the tonotopic gradient in the chicken cochlea. *Neuron* 19: 1061–1075, 1997.

Saito M, Nelson C, Salkoff L, and Lingle CJ. A cysteine-rich domain defined by a novel exon in a Slo variant in rat adrenal chromaffin cells and PC12 cells. *J Biol Chem* 272: 11710–11717, 1997.

Schreiber M and Salkoff L. A novel calcium-sensing domain in the BK channel. *Biophys J* 73: 1355–1363, 1997.

Spitzer NC and Lamborghini J. The development of the action potential mechanism in amphibian neurons. *Proc Natl Acad Sci USA* 73: 1641–1652, 1976.

Spitzer NC and Ribera AB. Development of electrical excitability in embryonic neurons: mechanisms and roles. *J Neurobiol* 37: 9585–9593, 1998.

Sun Q and Dale N. Developmental changes in expression of ion currents accompany maturation of locomotor pattern in frog tadpoles. *J Physiol* 507: 257–264, 1998.

Tian L, Duncan RR, Hammond MS, Coghill LS, Wen H, Rusinova R, Clark AG, Levitan IB, and Shipston MJ. Alternative splicing switches potassium channel sensitivity to protein phosphorylation. *J Biol Chem* 276: 7717–7720, 2001.

Tseng-Crank J, Foster CD, Krause JD, Mertz R, Godinot N, DiChiara TJ, and Reinhart PH. Cloning, expression, and distribution of functionally distict $Ca^{(2+)}$-activated K^{+} channels isoforms from human brain. *Neuron* 13: 1315–1350, 1994.

Vincent A, Lautermilch NJ, and Spitzer NC. Antisense suppression of potassium channel expression demonstrates its role in maturation of the action potential. *J Neurosci* 20: 6087–6094, 2000.

Wang ZW, Saifee O, Nonet ML, and Salkoff L. SLO-1 potassium channels control quantal content of neurotransmitter release at the *C. elegans* neuromuscular junction. *Neuron* 32: 867–881, 2001.

Weiger TM, Hermann A, and Levitan IB. Modulation of calcium-activated potassium channels. *J Comp Physiol [A]* 188: 79–87, 2002.

Xie J and Black DL. A CaMK IV responsive RNA element mediates depolarization-induced alternative splicing of ion channels. *Nature* 410: 936–939, 2001.

Xie J and McCobb DP. Control of alternative splicing of potassium channels by stress hormones. *Science* 280: 443–446, 1998.